

# Realistic Simulation of Transcranial Direct Current Stimulation via 3-D High-resolution Finite Element Analysis: Effect of Tissue Anisotropy

Hyun Sang Suh, *Student Member, IEEE*, Sang Hyuk Kim, *Student Member, IEEE*, Won Hee Lee, *Student Member, IEEE*, and Tae-Seong Kim, *Member, IEEE*

**Abstract**—Recently, transcranial direct current stimulation (tDCS) is getting an attentions as a promising technique with a capability of noninvasive and nonconvulsive stimulation to treat ill conditions of the brain such as depression. However, knowledge on how exactly tDCS affects the activity of neurons in the brain is still not sufficient. Precise analysis on the electromagnetic effect of tDCS on the brain requires finite element analysis (FEA) with realistic head models including anisotropy of the white matter and the skull. In this paper, we have simulated tDCS via 3-D high-resolution FEA and investigated the effect of tissue anisotropy on tDCS. The results show that the skull anisotropy induces a strong shunting effect, causing a shift of the stimulated areas, and the white matter anisotropy affects strongly the current flow directions, changing the current field distribution inside the human brain. Our presented methodology and results should be useful for more effective guiding and treatment using tDCS.

## I. INTRODUCTION

TRANSCRANIAL direct current stimulation is one of the noninvasive brain stimulation techniques by injecting weak direct current (usually 1-2mA) through the electrodes positioned on the patient's scalp. The cortical excitability depends on the polarity of stimulation generated by tDCS: anodal stimulation increases excitability, whereas cathodal stimulation is for inhibition. Inducing cortical excitability can be retained for at least one hour after the stimulation [1], [2].

Although tDCS is a promising tool for brain stimulation, there are still many factors to be considered for efficient and safe brain stimulation, such as electrode size and shape, duration of stimulation, and current intensity. To investigate the electromagnetic effect of tDCS on the human brain, finite element analysis (FEA) with realistic head models is the best methodology. In the previous works, simplified three-layer spherical head model [3], low-resolution head model [4], and only cigar-shaped white matter anisotropy [5] have been utilized without considering complicated geometry, variable anisotropic properties in the white matter, and shunting effect by the skull. For high-resolution FE head modeling of the head with optimal incorporation of white matter anisotropy

though diffusion tensors (DTs), we have recently developed an adaptive meshing technique called *wMesh* [6].

Through our adaptive meshing technique, in this study, we have performed realistic tDCS simulation to investigate the precise effect of tDCS on the brain stimulation. The electrical anisotropy was incorporated into both the skull and white matter regions. Especially for the white matter compartments, we have considered both a fixed-ratio [7] and variable-ratio [8] anisotropy settings.

Our results show that there are significant differences in the current field distribution, current flow, locations of stimulated areas, and focality of stimulation with respect to the skull and white matter anisotropy. The presented methodology and results should be useful for more effective guiding and treatment using tDCS.

## II. METHODS

### A. Generations of 3-D High-resolution FE Head Model

Our adaptive mesh generation process starts with the MRI-content adaptive mesh generation as reported as *cMesh* in [9]. Then high-density meshes in the white matter region are generated adaptively according the density of fractional anisotropy of DTs (i.e., *wMesh*) as detailed in [6]. Our automatic meshing techniques generate fast, automatic, and adaptive FE head models, allowing high-resolution FEA via commercial analysis packages like ANSYS [14].

In this work, our 3-D high-resolution *wMesh* full head model includes of 160,231 nodes and 1,009,447 tetrahedral elements. The whole head model consists of five regions of the head: namely, scalp, skull, white matter, gray matter, and cerebrospinal fluid (CSF) as indicated in color in Fig. 1.

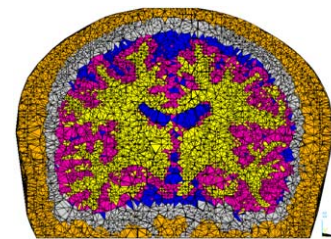


Fig. 1 Coronal view of the *wMesh* head model with 160,231 nodes and 1,009,447 tetrahedral elements: The five segmented sub-regions are shown in different colors (orange: scalp, gray: skull, magnetic red: gray matter, yellow: white matter and blue: CSF).

Manuscript received April 7, 2009.

Hyun Sang Suh, Sang Hyuk Kim, Tae-Seong Kim are with the Department of Biomedical Engineering, Kyung Hee University, Yongin, Gyeonggi, Republic of Korea (corresponding author to provide phone: +82-31-201-3731; fax: +82-31-201-3666; e-mail: [tskim@khu.ac.kr](mailto:tskim@khu.ac.kr)).

Won Hee Lee is with the Department of Biomedical Engineering, University of Minnesota.

### B. Isotropic and Anisotropic Conductivity Setup

In order to examine the effects of anisotropic conductivity of the tissue on tDCS, we have constructed three different models by assigning the anisotropic conductivity to the white matter and skull regions.

Model I consists of isotropic conductivity values for every region. We used isotropic electrical conductivity values from the literature as described in [10] and [11]. The isotropic conductivity values for the white matter, gray matter, CSF, skull, and scalp were set to be 0.14 S/m, 0.33, 1.79, 0.0132, and 0.33, respectively.

Model II includes anisotropic conductivity of white matter and skull with the fixed anisotropic ratio of 1:10 and isotropic conductivities for other regions: for the white matter, the electric conductivity in the parallel direction to neural fibers (or the main direction of diffusion tensor) is ten-time bigger than that in the normal direction; the conductivity in the tangential direction to the skull is ten times than that in the perpendicular direction. That is using the eigenvector and eigenvalues from DT-MRIs and according to the volume constraint algorithm [11], the conductivity in the longitudinal direction is 0.65 S/m and in the transverse direction is 0.065 in the white matter; the conductivity in radial direction is 0.002844 and in transverse direction is 0.02844 in the skull.

Model III is composed of the skull with its anisotropic conductivity setup with the fixed anisotropic ratio of 1:10, the white matter with the variable anisotropic ratio [8], and isotropic conductivities for other regions. To represent the white matter anisotropic property more realistically, we used the Tuch's effective medium approach method [8] to generate the eigenvalue of white matter: this method states that strong linear relationship of eigenvalue of diffusion tensor and conductivity tensor in the white matter and could be written as

$$\frac{d_1}{\sigma_1} = \frac{d_2}{\sigma_2} = \frac{d_3}{\sigma_3} \quad (1)$$

where  $d_1$ ,  $d_2$ , and  $d_3$  are eigenvalues of the diffusion tensor.  $\sigma_1$ ,  $\sigma_2$ , and  $\sigma_3$  are the eigenvalues of the conductivity tensor at each voxel of the white matter. Using the volume constraint, we obtained anisotropic conductivity tensor of the white matter with the variable anisotropic ratio.

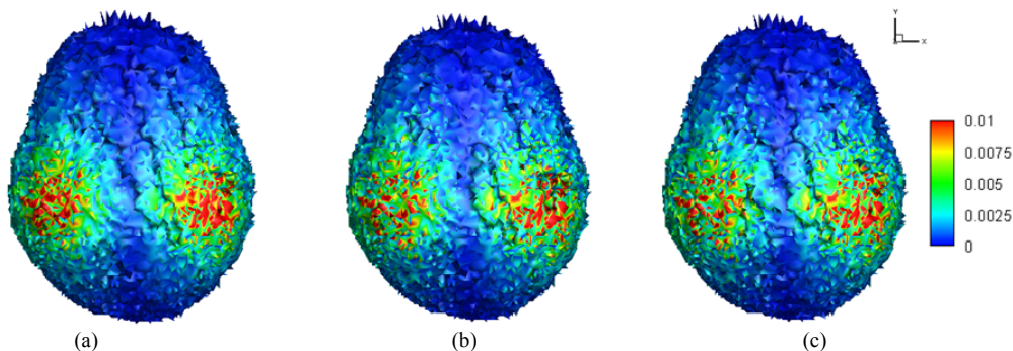


Fig. 2 Distribution of electric field on the brain surface from (a) the isotropic head model, (b) the anisotropic head model with fixed anisotropic ratio of 1:10, and (c) the anisotropic head model with variable anisotropic ratio.

### C. tDCS Simulation

An anode electrode was placed at C3 and a cathode electrode was placed at C4 (according to the standard of the international 10/20 EEG system) to stimulate the motor cortex and induce the electric field in the brain [12]. The bipolar electrodes were modeled using two nodes of the mesh as point electrodes, where 1mA total constant current was injected at the activating electrode. The induced electric field in the head by tDCS was computed by solving the following quasi-static Laplace equation.

$$\nabla \cdot (\sigma \nabla V) = 0 \quad (2)$$

where  $V$  and  $\sigma$  represent the electric potential and the electrical conductivity respectively. We acquired the induced electric field using the sparse direct equation solver in ANSYS based on the direct elimination of equations.

### D. Evaluation Criteria for tDCS

To compare the influence of anisotropic conductivity in the white matter and skull on the effects of tDCS, we evaluated several properties of the induced electric field differences including (i) distribution of electric field intensity on the brain surface, (ii) distribution of electric field intensity and vector flow at some coronal planes of the brain, (iii) streamlines of electric field from the anode electrode to the cathode electrode, and (iv) parallelity between the induced electric field direction and the eigenvector of longitudinal direction in the white matter.

## III. RESULT

The distribution of the resulting electric field intensity on the brain is shown in Fig. 2. The color bar of electric field distribution is set from 0 to 0.01mV/m. In the isotropic head model, the induced electrical field seems more focal and strong right under the stimulating electrodes, but in the anisotropic cases, the field seems more diffused and there is a shift in the high intensity regions. These results suggest the skull and white matter anisotropy affects the focality and the brain regions under stimulation.

In Fig. 3, we show the distribution of electric field intensity and current flow projected onto a coronal plane. In the isotropic model, we can observe the uniform current flow from the activating (i.e., injecting) electrode to the reference

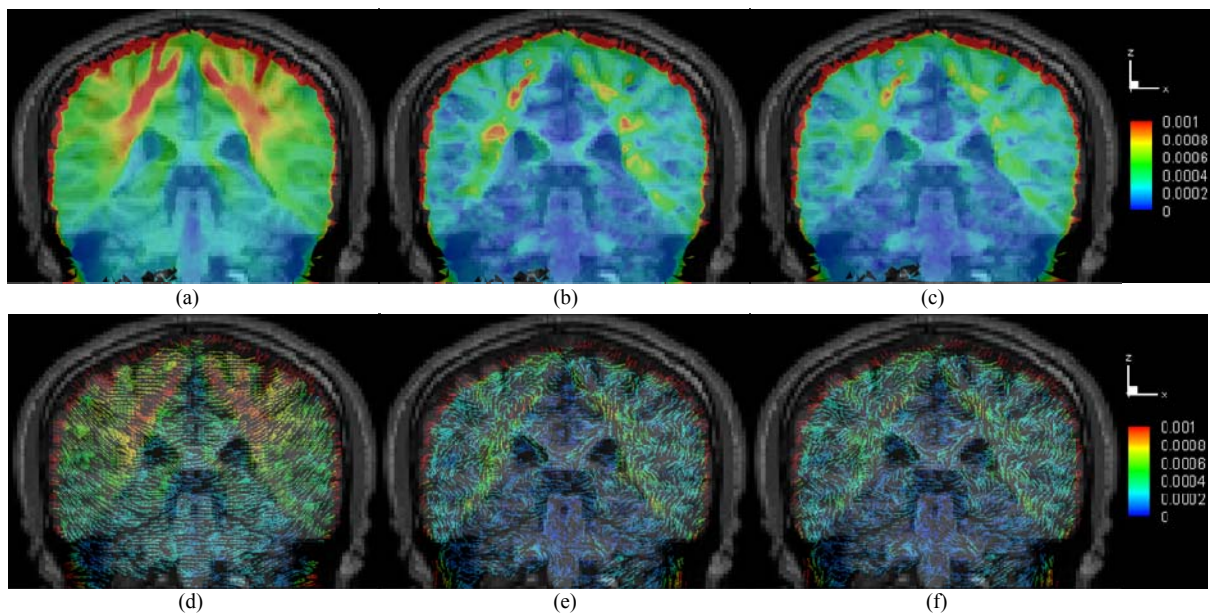


Fig. 3 Visualization of the electric field intensity and vector flow within brain region overlaid on the T1-MRI coronal slice through both electrodes. The first row displays the electric field intensity. The second row displays the electric field vector flow. (a), (d) the isotropic head model, (b), (e) anisotropic head model with fixed anisotropic ratio of 1:10 and (c), (f) anisotropic head model with variable anisotropic ratio.

(i.e., exiting) electrode and the degree of induced current densities, whereas the two anisotropic models have inhomogeneous current flow and more diffused intensities. We believe this is because of the shunting effect of the anisotropic skull (thus, less current being injected into the brain) and the anisotropic white matter affects the current flow (thus, diffusing electrical field). We have noticed also some differences between Model II and III: the white matter region in the anisotropic model II has higher intensity than the model III, otherwise both models have similar results.

Fig. 4 shows how parallel the electric field is to the main direction of the white matter: the color is coded from 0 (less parallel: cyan) to 1 (highly parallel: red). The main nerve fiber direction is indicated using line segments in white. In the isotropic head model, as the colors indicate the electrical field is not parallel to the main directions of anisotropy (i.e., main diffusion directions or nerve fiber directions), whereas in the anisotropic models, as expected, the direction of the field and white matter is highly parallel.

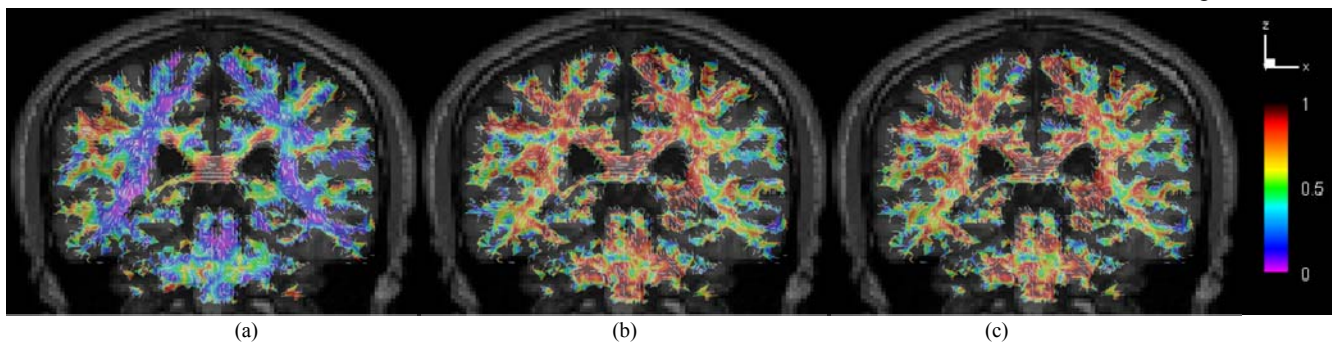


Fig. 4 Parallellity between induced electric field direction and nerve fiber direction in the white matter on the T1-MRI coronal slice through both electrodes: (a) the isotropic head model, (b) anisotropic head model with fixed anisotropic ratio of 1:10 and (c) anisotropic head model with variable anisotropic ratio.

Fig. 5 shows the streamline of the electric field starting from the anode to the cathode electrode, we set up two streamlines through an arbitrary point in the white matter. The streamlines indicate current flow differences in each model. In comparison with the isotropic model, we can observe more divergent current flow along the scalp due to the shunting effect by the anisotropic skull.

#### IV. DISCUSSION AND CONCLUSION

The purpose of this paper is to examine the effect of tDCS with realistic high-resolution FEA including most realistic tissue anisotropy: we used the high-resolution FE conductivity models with the different anisotropic setup. The simulation results suggest that tissue anisotropy has significant effects on the stimulation in the deeper brain areas. Without the consideration of tissue anisotropy, the effect of tDCS in the isotropic model seems to match well with our understanding of general electromagnetic analysis: isotropic current field and its flow. However, in the anisotropic models,

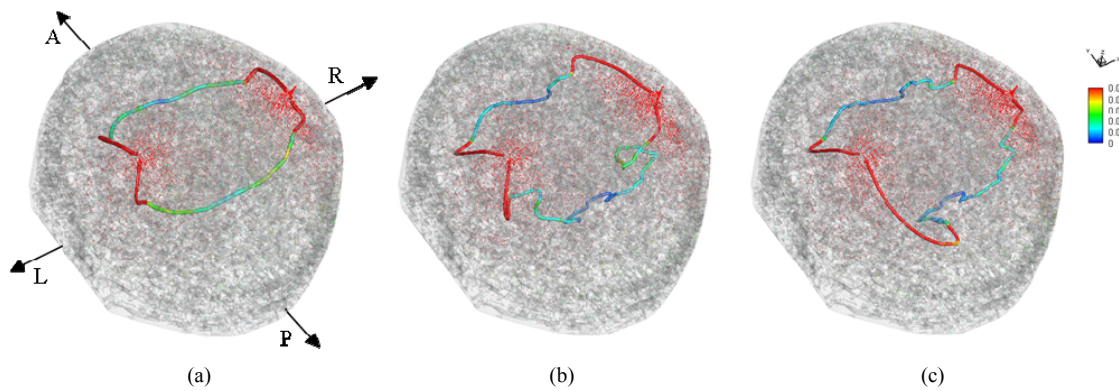


Fig. 5 Streamline of electric field vector from the anode to the cathode (A: anterior, P: posterior, R: right, L: left): (a) the isotropic head model, (b) the anisotropic head model with fixed anisotropic ratio of 1:10 and (c) the anisotropic head model with variable anisotropic ratio

our high-resolution FEA reveals significantly different results.

Our analysis also indicates that required injection current to produce a 0.31 mV/mm at the cortical surface right under the anode is 0.5mA in the isotropic, 2.02 in the fixed anisotropic and 2.39 in the variable anisotropic case respectively, requiring much stronger stimulation if the tissue anisotropy is considered. As we mentioned above, we also examined the patterns of parallelity between the field and the main eigenvector of conductivity tensor in the white matter. There are remarkable differences between the isotropic and anisotropic cases. These patterns are important factors to be considered in the determination of tDCS electrodes position, since current flow along the direction of fiber affects strongly on the efficacy and safety of tDCS.

There are some limitations on our tDCS model in the present study. We used point the source electrode instead of commercial pad electrode. The skull was modeled with one compartment, but realistic human skull is made of three sub-regions, one soft bone layer surrounded by two hard bone layer, which have different conductivities [13]. Nevertheless, our results suggest that one should optimize, for efficient and safe tDCS treatment, location, configuration, and the number of electrodes with minimal current and high spatial focality in order to effectively simulate target areas with maximum intensity but non-target areas with minimum intensity.

We believe that our methodology and the presented results should help to elucidate the induced stimulation effect on the brain via tDCS and should be useful for further investigation of more effective tDCS.

#### ACKNOWLEDGMENT

This work was supported by the Korea Science and Engineering Foundation (KOSEF) grant funded by the Korea government (MEST) (2009-0075462).

#### REFERENCES

- [1] M. A. Nitsche and W. Paulus, "Excitability changes induced in the human motor cortex by transcranial direct current stimulation," *J. physiol.*, vol 527.3, pp. 633-639, 2000.
- [2] M. A. Nitsche, D. Liebetanz, N. Lang, A. Antal, F. Tergau, and W. Paulus, "Safety criteria for transcranial direct current stimulation (tDCS) in humans," *Clin Neurophysiol.*, vol 114, pp. 2220-2222, 2003.
- [3] A. Datta, M. Elwassif, F. Battaglia, and M. Bikson, "Transcranial current stimulation focality using disc and ring electrode configuration: FEM analysis," *J. Neural Eng.*, vol 5, pp. 163-174, 2008.
- [4] C. Im, H. Jung, J. Choi, S. Y. Lee, and K. Jung, "Determination of optimal electrode position for transcranial direct current stimulation (tDCS)," *Phys. Med. Biol.*, vol 53, pp. N219-N225, 2008.
- [5] T. F. Oostendorp, Y. A. Hengeveld, C. H. Wolters, J. Stinstra, G. V. Elswijk, and D. F. Stegeman, "Modeling transcranial DC stimulation," *IEEE EMBS*, Vancouver, Canada, August 20-24, 2008.
- [6] W. H. Lee, T. -S. Kim, A. T. Kim, and S. Y. Lee, "3-D diffusion tensor MRI anisotropy content-adaptive finite element head model generation for bioelectromagnetic imaging," *IEEE EMBS*, Vancouver, Canada, August 20-24, 2008.
- [7] P. W. Nicholson, "Specific impedance of cerebral white matter," *Exp. Neurol.*, vol. 13, pp. 386-401, 1965.
- [8] H. Hallez, B. Vanrumste, P. V. Hese, S. Delputte, and I. Lemahieu, "Dipole estimation errors due to differences in modeling anisotropic conductivities in realistic head models for EEG source analysis," *Phys. Med. Biol.*, vol. 53, pp 1877-1894, 2008.
- [9] W. H. Lee, T. -S. Kim, M. H. Cho, Y. B. Ahn, and S. Y. Lee, "Methods and evaluations of MRI content-adaptive finite element mesh generation for bioelectromagnetic problems," *Phys. Med. Biol.*, vol. 51, pp. 6173-6186, 2006.
- [10] S. Kim, T. -S. Kim, Y. Zhou, and M. Singh, "Influence of conductivity tensors on the scalp electrical potential: Study with 2-D finite element models," *IEEE Trans. Nucl. Sci.*, vol. 50, pp. 133-138, 2003
- [11] C. H. Wolters, A. Anwander, X. Tricoche, D. Weinstein, M. A. Koch, and R. S. Macleod, "Influence of tissue conductivity anisotropy on EEG/MEG field and return current computation in a realistic head model: A simulation and visualization study using high-resolution finite element modeling," *NeuroImage*, vol. 30, pp. 813-826, 2006.
- [12] S. Hesse, C. Werner, E. M. Schonhardt, A. Bardeleben, W. Jenrich, and S. G. B. Kirker, "Combined transcranial direct current stimulation and robot-assisted arm training in subacute stroke patients: A pilot study," *Restor. Neurol. Neurosci.*, vol. 25, pp. 9-15, 2007
- [13] R. J. Sadleir, and A. Argibay, "Modeling skull electrical properties," *Ann. Biomed. Eng.*, vol. 35, pp. 1699-1712, 2007
- [14] ANSYS. Available: <http://www.ansys.com/>